Electronic Supplementary Material (ESI) for Physical Chemistry Chemical Physics.

Supporting Information

Unraveling the low-temperature activity of Rh-CeO_2 catalysts in CO oxidation: probing the local structure and Red-Ox transformation of Rh^{3+} species

Elizaveta A. Fedorova*,[1] Tatyana Yu. Kardash*,[2] Lidiya S. Kibis,[2] Olga A. Stonkus,[2] Elena M. Slavinskaya,[2] Valery A. Svetlichnyi,[3] Simone Pollastri,[4] Andrei I. Boronin[2]

[1]Leibniz Institute for Catalysis, Albert-Einstein Str. 29a, 18059, Rostock, Germany
[2]Boreskov Institute of Catalysis, pr. Lavrentieva 5, 630090, Novosibirsk, Russia
[3]Tomsk State University, pr. Lenina 36, 634050 Tomsk, Russia
[4]Elettra-Sincrotrone Trieste S.C.p.A., Strada Statale 14, km 163.5, Basovizza, Trieste, I-34149, Italy

Corresponding Authors

*e-mail: Elizaveta.Fedorova@catalysis.de; kardash@catalysis.ru

Estimation of the influence of mass transport and heat transfer limitation in the range of low CO conversion (below 15%).

To eliminate the possible influence of the mass transport and heat transfer limitation on the calculated values of the rate of the catalytic reaction we performed the corresponding estimations following the procedure described in works [1-3].

To estimate the influence of the internal diffusion we checked the Weisz modulus (Φ):

$\Phi = \frac{r_{obs} \times \rho_p \times d_p^2}{D_{eff} \times C_{CO}^{bulk}}$, where r_{obs}= observed reaction rate, mol/kg_{cat}·s; ρ_p = bulk density of catalyst bed, kg/m^3;
d_p = catalyst particle diameter, 0.2 mm; D_{eff} = effective diffusivity, m^2/s; and C_{CO}^{bulk} = bulk gas concentration of CO, mol/m^3 (calculated as $C_{CO}^{bulk} = \frac{P_{CO}}{Rg \times T}$, P_{CO}= 202.6 Pa, R_g= gas constant (8.314 J/mol·K), T = reaction temperature, K).

The corresponding parameters for the 5Rh-CeO_2 and 1Rh-CeO_2 catalysts are given in Table S1. The resulted Φ value was 0.79 and 0.88, so, internal diffusion limitations can be discarded in accordance with the Weisz criterion (Φ<1).

To estimate the influence of the external diffusion we compared the bulk gas concentration of CO (C_{CO}^{bulk}) with the difference of CO concentration over the gas film (ΔC_{CO}):

$\Delta C_{CO} = \frac{r_{obs} \times d_p^2 \times \rho_p}{6 \times Sh \times D_{AB}}$, where r_{obs}= observed reaction rate, mol/kg_{cat}·s; d_p = catalyst particle diameter, 0.2 mm; ρ_p = bulk density of catalyst bed; D_{eff} = effective diffusivity, m^2/s; Sh is the Sherwood number, D_{AB}=the binary gas diffusivity, m^2/s.

The calculated value ΔC_{CO} =1.04×10^{-4} and 1.1×10^{-4} << C_{CO}^{bulk}, thus, the external diffusion limitations can be discarded.

Table S1. Calculated parameters for internal and external diffusion.

Sample	r_{obs}, mol/kg_{cat}·s	ρ_p, kg/m^3	D_{eff}, m^2/s	T, K	C_{CO}^{bulk}, mol/m^3	Sh	D_{AB} m^2/s	Φ	ΔC_{CO}, mol/m^3
5Rh-CeO_2	4.574×10^{-4}	1888	1.348×10^{-7}	300	8.12×10^{-2}	1.5	3.7×10^{-5}	0.79	1.04×10^{-4}
1Rh-CeO_2	4.854×10^{-4}	1888	1.422×10^{-7}	333	7.32×10^{-2}	1.5	3.7×10^{-5}	0.88	1.1×10^{-4}

To estimate the heat transfer limitations, we used the Mear's criterion [2,3].

$C_M = \left| \frac{-\Delta H r_{obs} \rho_p d_p E_a}{2hT^2 R_g} \right| < 0.15$, where ΔH= heat of reaction, kJ/mol; E_a = activation energy, kJ/mol; h=heat transfer coefficient between gas and pellet, kJ/m^2·s·K, R_g= gas constant (8.314 J/mol·K), T = reaction temperature, K

The corresponding parameters for the 5Rh-CeO_2 and 1Rh-CeO_2 catalysts are given in Table S1, TableS2. The calculated value C_M =4.67×10^{-3} and 4.16×10^{-3} << 0.15, thus we can neglect the heat transfer effect during the kinetic experiments.

Table S2. Calculated parameters for heat transfer.

Sample	ΔH, kJ/mol	E_a, kJ/mol	h, kJ/m²·s·K	T, K	C_M
5Rh-CeO_2	-283	38.9	6.5×10^{-2}	300	0.00467
1Rh-CeO_2	-283	40.2	6.5×10^{-2}	333	0.00416

The adiabatic heating was also estimated. For the 5Rh-CeO_2 and 1Rh-CeO_2 catalysts the CO conversion 15% is reached at 27 and 60°C, respectively. For this temperature the adiabatic heating can be calculated as: $\Delta T_{ad} = \Delta H\, C/(c_p \rho)$, where ΔH - heat of reaction, kJ/mol, C– reacted CO concentration = 0.013 mol/m³, c_p– specific heat = 1.043 (1.044) kJ/(kg deg), ρ– gas density - 1.123 (1.021) kg/m³ at 27 (57) °C.

The calculated value ΔT_{ad}= 3.2°C and 3.6°C, thus, adiabatic heating at 27 and 57°C does not exceed 3.2 and 3.6°C.

[1] P.-A. Carlsson, V.P. Zhdanov, M. Skoglundh, *Phys. Chem. Chem. Phys.*, 2006, **8**, 2703-2706.

[2] A.I. Boronin, E.M. Slavinskaya, A. Figueroba, A.I. Stadnichenko, T.Y. Kardash, O.A. Stonkus, E.A. Fedorova, V.V. Muravev, V.A. Svetlichnyi, A. Bruix, K.M. Neyman, *Appl. Catal. B: Environ.*, 2021, **286**, 119931.

[3] H.-H. Liu, Y. Wang, A.-P. Jia, S.-Y. Wang, M.-F. Luo, J.-Q. Lu, *Appl. Surf. Sci.*, 2014, **314**, 725-734.

Table S3. Structural and microstructural characteristics of ceria in the Rh-CeO_2 catalysts, TOF at 25°C and activation energy (E_a). a - is lattice parameter, D – is average crystallite size, e_0 - is microstrains of CeO_2 lattice.

Sample	a, Å	D, nm	e_0, %	S, m^2/g	TOF*10^3, s^{-1}	E_a, kcal/mol
CeO_2	5.416(1)	7.3(3)	0.10(2)	122	-	-
1Rh-CeO_2	5.411(1)	6.6(3)	0.12(3)	145	0.90	9.6
5Rh-CeO_2	5.403(2)	7.2(3)	0.18(3)	138	0.86	9.3

Table S4. Results of the fittings Rh K-edge EXAFS of the 5Rh-CeO_2 sample.

Sample	Type	R (Å)	σ^2 ($Å^2$)	CN	ΔE_0 (eV)	R_f (%)	Rh^0 fraction*
init	Rh-O	2.046 (2)	0.0040 (2)	5.5 (1)	-3.2 (4)	0.54	-
	Rh-O-Rh	3.072 (7)	0.0078 (7)	2.0 (2)			
	Rh-O-Ce	3.18 (2)	0.007 (2)	0.7 (3)			
Red-Ox	Rh-O	2.034 (2)	0.0049 (3)	5.3 (1)	-4.0 (4)	0.82	-
	Rh-O-Rh	3.068 (6)	0.0074 (6)	2.1 (2)			
	Rh-O-Ce	3.15 (1)	0.007 (1)	0.7 (1)			
Red	Rh-O	2.028 (2)	0.0042 (3)	4.4 (1)	-4.7 (4)	0.99	0.18 (1)
	Rh-Rh	2.65 (1)	0.013 (1)	2.0 (3)			
	Rh-O-Rh	3.09 (1)	0.008 (1)	0.9 (2)			
	Rh-O-Ce	3.20 (1)	0.005 (1)	0.5 (1)			

*Data were obtained by fitting of the XANES spectra of the 5Rh-CeO_2 catalysts with a linear combination of the XANES spectra of Rh foil and the Rh-CeO_2-init sample like a reference of Rh metal and Rh^{3+} highly dispersed spices on CeO_2, respectively.

CN=coordination number

Table S5. Hydrogen consumption during TPR-H_2

Sample	T_{max}-1, °C	T_{max}-2, °C	H_2 consumed, µmol/g	H_2/Rh
1Rh-CeO_2	-	100	672	6.9
5Rh-CeO_2	32	75	1740	3.3

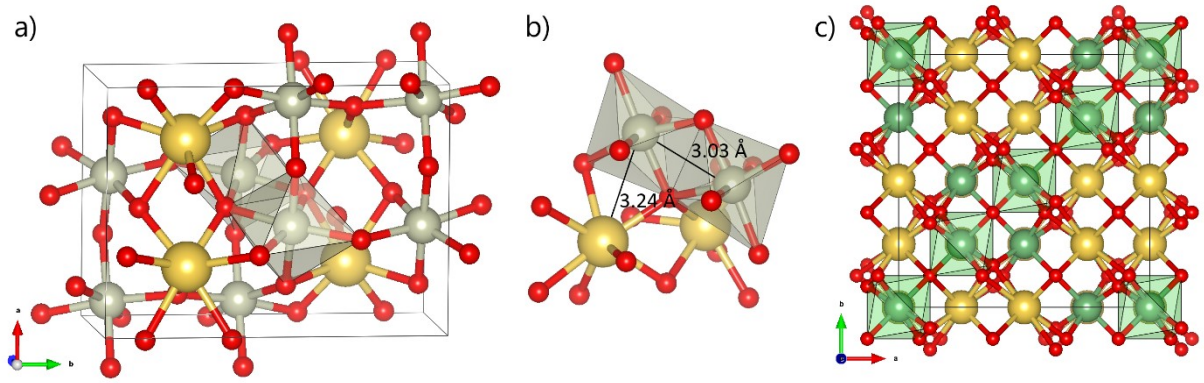

Figure S1. (a) Unit cell and (b) local structure of $CeRh_2O_5$ oxide; (c) unit cell of $Ce_2Zr_2O_7$ oxide with pyrochlore structure. Ce – yellow, Rh – gray, Zr – green, O – red.

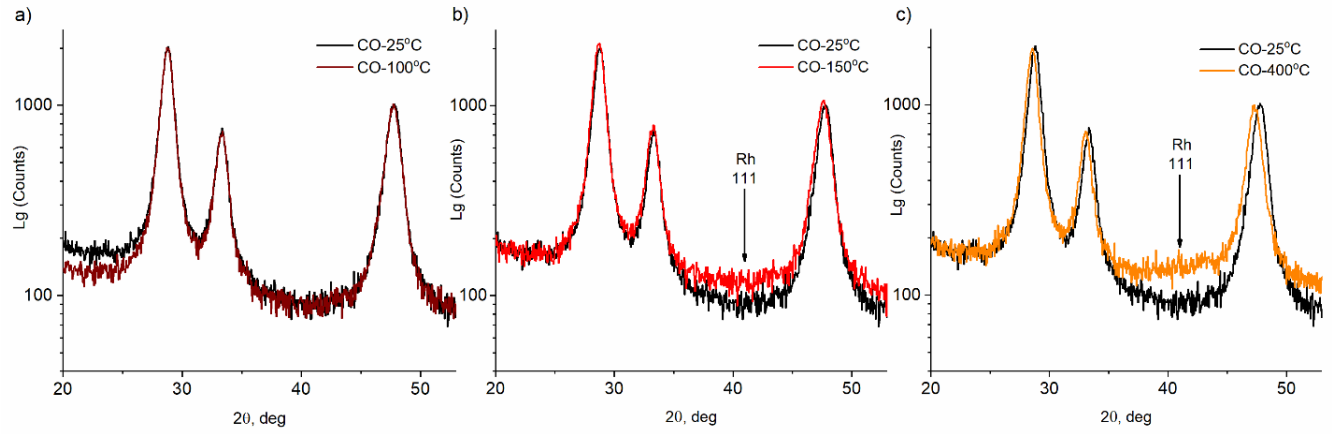

Figure S2. Comparison of the in situ XRD pattern of 5Rh-CeO_2 catalyst in CO collected at 25°C with in situ XRD patterns in CO collected at 100°C (a), 150°C (b) and 400°C.

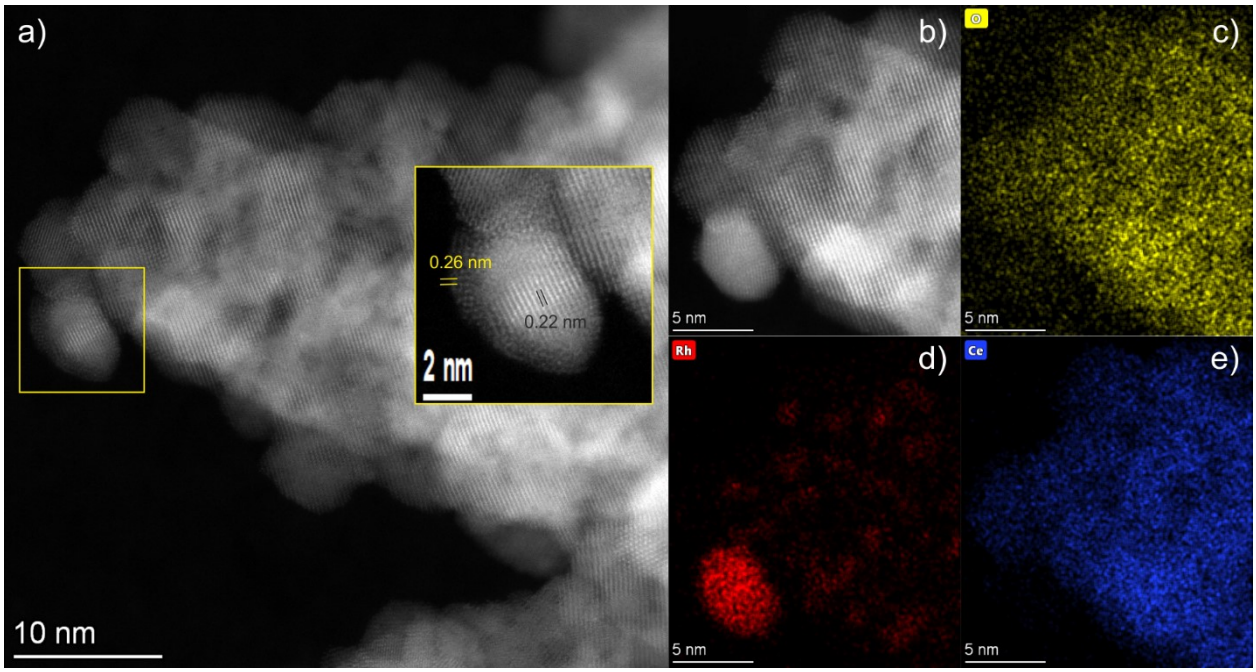

Figure S3. TEM data for the 5Rh–CeO_2 sample after the TPR-CO experiment: (a, b) HAADF-STEM image, EDX-mapping patterns showing distribution of (c) O (yellow color), (d) Rh (red color), (e) Ce (blue color) in area (b). The inset in figure (a) shows a magnified image of a core@shell Rh@RhO_x nanoparticle with indication of interplanar distances. The oxidized "shell" layer disappeared during the EDX acquisition (figure b) due to reduction under the action of electron beam.

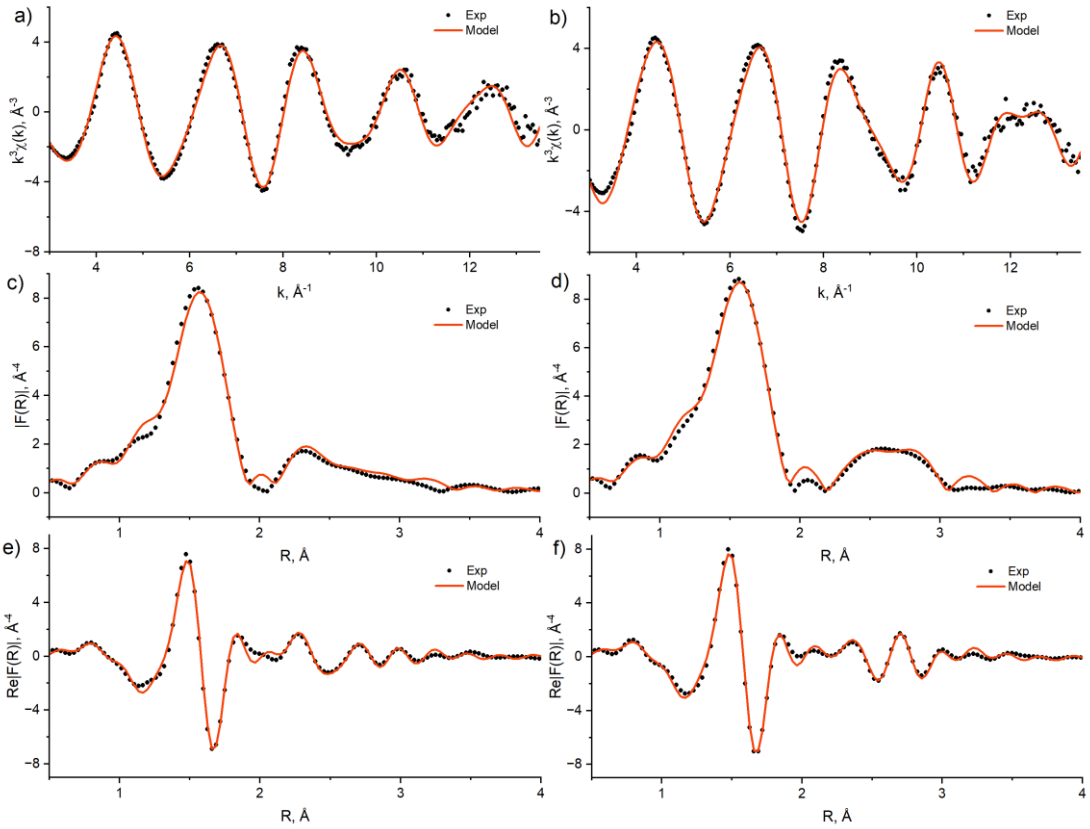

Figure S4. Rh K-edge k^3-weighted (a, b) χ(k) EXAFS spectra and its Fourier transformed (c, d) magnitude and (e, f) real part for the 5Rh-CeO_2 sample after (a, c, e) TPR-CO experiment (Red) and after (b, d, f) TPR-CO experiment followed by TPO experiment (Red-Ox). Experimental curves - black dots; corresponding fits - solid red curves.

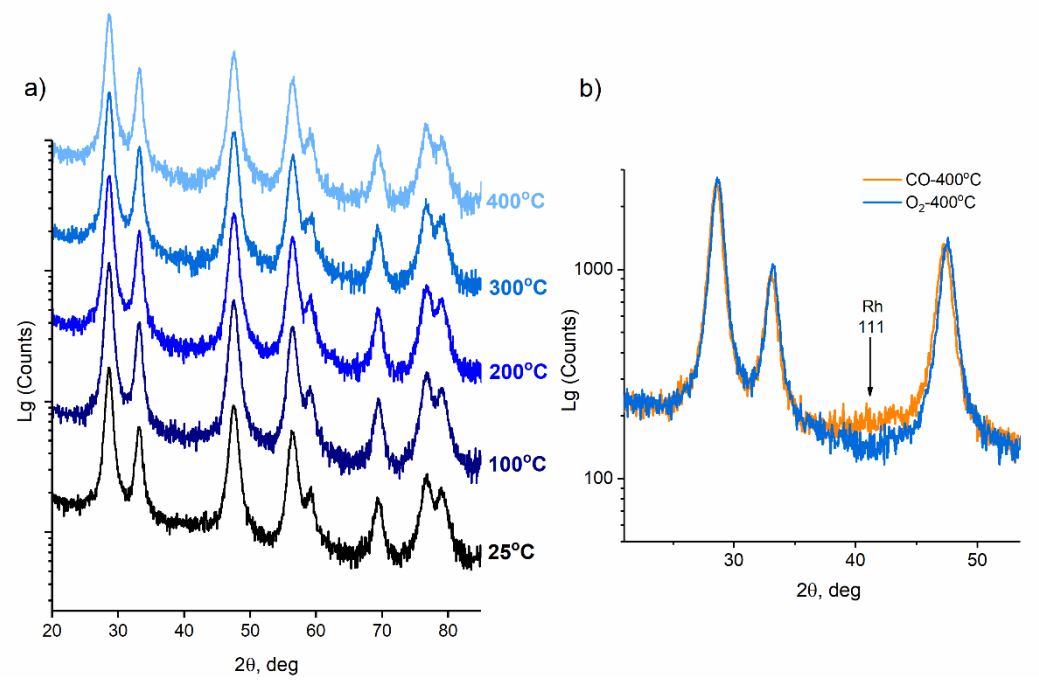

Figure S5. (a) In situ XRD patterns of the 5Rh-CeO_2 catalyst O_2 exposure. (b) Comparison of the in situ XRD pattern of the 5Rh-CeO_2 catalyst in CO at 400°C with in situ XRD pattern of the sample in O_2 at 400°C. After reoxidation Rh metal reflection disappeared, which indicates oxidation of Rh metal nanoparticles.